IET Renewable Power Generation

Special Issue Call for Papers

Be Seen. Be Cited.
Submit your work to a new IET special issue

Connect with researchers and experts in your field and share knowledge.

Be part of the latest research trends, faster.

Read more

The Institution of Engineering and Technology

Received: 18 February 2021 | Revised: 26 July 2021 | Accepted: 24 August 2021

IET Renewable Power Generation

DOI: 10.1049/rpg2.12285

The Institution of Engineering and Technology WILEY

ORIGINAL RESEARCH PAPER

Analysis of the Caribbean wave climate for wave energy harvesting

Kevin G. Lemessy | **Krishpersad Manohar** | **Anthony Adeyanju**

Faculty of Engineering, The University of the West Indies, St. Augustine, Trinidad and Tobago, West Indies

Correspondence
Krishpersad Manohar, Mechanical and Manufacturing Engineering Department, Faculty of Engineering, The University of the West Indies, St. Augustine, Trinidad and Tobago, West Indies.
Email: krishpersad.manohar@sta.uwi.edu

Abstract

In this study, the design requirements for a regional wave energy converter are identified from the analysis of 10 years of spectral data provided by nine buoys located across the Caribbean. It indicated that the average significant wave height and wave period in the Caribbean is 1.62 m and 5.91 s, respectively, while the average total theoretical power capable of being absorbed from a wave energy converter is 7.4 kilowatts per meter of surface waves. Devices should be designed to withstand a significant wave height of 19.0 ± 2.8 meters (95% confidence) for a 1 in 100 year return wave. This was determined by performing various extreme wave analyses. Additionally, a design life of 30 years for a device would have a probability of exceedance regarding this return wave as 26%. Using two-dimensional wave spectra analysis for the resource study, the overall spectral width, directionality coefficient and direction of the maximum directionally resolved wave power for the region are determined to be 0.172, 0.74 and 42°, respectively. It is expected that the combination of these information would improve the viability of a wave energy industry in the Caribbean and advance technological development.

1 | INTRODUCTION

1.1 | Background

Currently,members of the United Nations have been working studiously across the world towards the attainment of the UN 2030 Agenda for Sustainable Development. This agenda takes many forms as there are 17 main goals being addressed. Of particular importance to this paper is Goal No. 7, which is entitled "Ensure access to affordable, reliable, sustainable and modern energy for all" [1]. According to the United Nations [1], the 2030 agenda specifically targets worldwide access to affordable, dependable and contemporary energy systems, a drastic increase of renewable energy to the global supply, and the development/advancement of infrastructure and technology to support modern sustainable energy services in Small Island Developing States (SIDS). The Caribbean region is a perfect example of the SIDS being referenced by the United Nations [1].

In 2019, Lemessy, Manohar and Adeyanju [2] conducted a comparative analysis of "notable wave energy countries" to Caribbean SIDS using developed metrics such as coastline per area ratio and maritime economic activity, amongst others. The paper suggests that SIDS (such as the Caribbean nations) is well suited for a marine renewable energy industry when juxtaposed against "active wave energy countries". However, as one begins to consider the development of wave energy converters for this region, there is an unfortunate gap in literature with respect to resource characterisation that creates a barrier for technological advancement. Lemessy, Manohar and Adeyanju [3] expressed that the lack of information regarding wave energy resource in many countries is a key challenge experienced by the industry globally.

Wave energy research continues to be developed as individuals across the world seek to find the most amenable generator and means to capture and efficiently convert the energy into electricity. One such advancement is the work put into wave energy park optimisation. Göteman, et al. [4] indicated, "optimal layouts will position the WECs along lines perpendicular to wave direction at sites with a narrow interval of incident wave directions". This detail expresses the passion of this study as Göteman, et al. [4] went on to explain that though other criteria such as viscosity and rotation are critical elements of fluid properties, it is not feasible to be considered in modelling of wave energy parks. However, knowledge of wave directionality and wave propagation is paramount over a long period for the design of parks.

UNITS: J, Joules; kg, Mass; m, Meters; s, Seconds; W, Watts

In the past, many studies attempted to predict wave behaviour across different regions of the world. Muzathik, et al. [5] identified the Gumbel distribution as one of the many distributions that could predict extreme wave heights, while Mathiesen, et al. [6] expressed their belief that most wave climates follow the Weibull distribution. Information regarding the distribution preference of the extreme Atlantic Ocean waves in the Caribbean is not currently identified in literature. An extreme wave analysis must be conducted so that the appropriate structural design loads are considered, minimising the failure of wave energy converters (WEC) due to storm events [7].

There has been some relative work done in the Caribbean region that deserves special mention; this includes spectral widths and directionality coefficients by Ahn, Haas and Neary [8]; wave energy by Ahn and Neary [9]; equator friendly WECs by Henry, et al. [10]; and wave climate trends by Appendini, et al. [11], to name a few. However, there is no substantive study regarding wave characterisation found in literature for the Atlantic ocean aspect of the Caribbean region in the context of WECs. The wave climate in the Caribbean Sea and the Gulf of Mexico is much different from the climate positioned on the Atlantic side.

Critical information regarding the characteristics of the wave climate must be easily attainable by developers for suitable designs of wave energy converters and systems. As such, there is a desperate need for an expansive continuous resource analysis to be conducted in the Caribbean region if a marine energy industry is to develop. This paper seeks to research and provide design criteria, such as the average significant wave height, the average wave period and the average total theoretical power. Developers need this information specifically for the design of the energy absorption mechanism, amongst other elements like the Power Take-Off system. Additional metrics including the spectral width (for frequency sensitive WECs), directionality coefficient (for WECs that prefer a steady wave power direction) and direction of the maximum directionally resolved wave power (to guide developers on how to position fixed WECs for maximum efficiency) are also determined. The details under extreme conditions are also a key element of the study, as it would guide developers on the selection of materials and dimensional characteristics of device components to improve device survivability. According to IEC [12] and IEC [13], this information will lay the foundation for the development of relevant and noteworthy wave energy converters.

1.2 | Geographical location

The Caribbean region is a chain of islands located to the right of Central America, south of North America and to the north of South America. It is bordered by the Gulf of Mexico, the Atlantic Ocean and the Caribbean Sea (Figure 1). The National Oceanic and Atmospheric Administration (NOAA) has strategically located data collecting buoys in the region that feeds into the National Data Buoy Centre (NDBC). The plethora of buoys spread over the Atlantic Ocean and Caribbean Sea (Figure 1) currently has the ability to measure atmospheric pressure, wind direction, wind speed, gust, air temperature, water temperature, wave energy spectra, water-column height, relative humidity, ocean current velocity, precipitation, salinity, solar radiation, visibility, water level and water quality. However, some of the buoys do not provide the full spectrum of data [14].

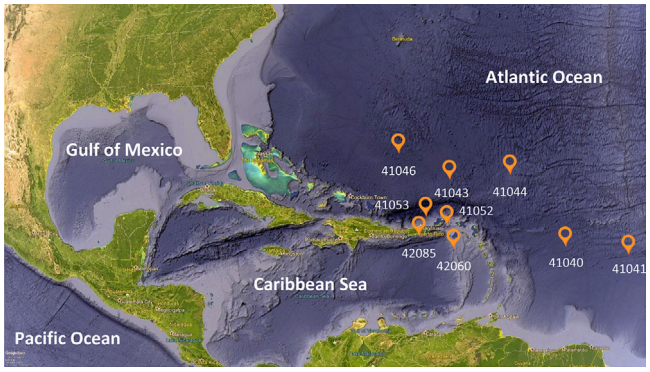

FIGURE 1 Image of the Caribbean region and approximate locations of the buoys (Image Courtesy Google Earth Pro)

2 | MATERIAL AND METHODS

To develop the design data for a Caribbean focused WEC, records from the National Oceanic and Atmospheric Administration (NOAA) [15] and National Data Buoy Centre were surveyed. The buoys selected were mainly on the Atlantic Ocean side of the Caribbean islands since this side is expected to be the most energetic region of the Caribbean (Figure 1). The results from each of the buoys deployed were scrutinized to determine whether they had a reasonable amount of data spanning 10 years. The following selected buoys met the 10-year (2009 and 2018) minimum data criteria for this study: 41040, 41041, 41043, 41044, 41046, 41052, 41053, 42060 and 42085.

The identified buoys are dispersed in the region (from 14° N to 24° N and 46° W to 69° W) in a manner that will allow them to measure ocean swells and localised wind waves from different bodies of water. Buoys 41040, 41041, 41043, 41044, 41046, 41052 and 41053 are recording data from waves originating in the Atlantic Ocean, while buoys 42085 and 42060 are recording localised wind waves from the Caribbean Sea. Buoys 41052, 41053 and 42085 have an average depth of 31 m; therefore, they can be considered to be observing the nearshore wave climate, while the buoys 41040, 41041, 41043, 41044, 41046 and 42060 are observing the offshore wave environment. The mix of nearshore, offshore, Atlantic borne and Caribbean Sea generated waves, gives the study more rigour in its attempt to investigate the general wave climate of the Caribbean region.

The data for each buoy over the selected 10-year period was systematically downloaded, organised and refined. This involved deleting data that represented values when the buoys did not have any measured information. It was easily identifiable as it is characterised by seeing a significant wave height of 99 m or wave period of 99 s, a code used for missing data according to [16]. This resulted in only 668,294 of the 2,183,509 wave

TABLE 1 Individual buoy details obtained during the period 2009–2018 [15]

Station	41040	41041	41043	41044	41046	41052	41053	42060	42085
Depth (m)	5106	3485	5289	5391	5430	44	32	1525	17
Location – latitude (° North)	14.559	14.329	21.132	21.597	23.832	18.250	18.474	16.387	17.860
Location – longitude (° West)	53.073	46.082	64.856	58.621	68.417	64.763	66.099	63.350	66.524
High. sig. wave height (m)	6.34	8.55	13.42	11.79	14.81	7.90	6.00	9.37	4.30
Low. sig. wave height (m)	0.54	0.53	0.02	0.32	0.01	0.20	0.10	0.31	0.20
Avg. sig. wave height (m)	2.00	2.03	1.81	1.87	1.74	1.05	1.27	1.34	1.02
Avg. wave energy density per unit area of surface waves (J/m^2)	2,453	2,527	2,009	2,144	1,856	676	989	1,101	638
Maximum wave energy density per unit area of surface waves (J/m^2)	24,645	44,821	110,422	85,227	134,480	38,265	22,073	53,830	11,337

TABLE 2 Average wave climate details across the Caribbean region from 2009 to 2018 [15]

Year	2009	2010	2011	2012	2013	2014	2015	2016	2017	2018	Avg.
Average depth (m)	2924	2924	2924	2924	2924	2924	2924	2924	2924	2924	2924
High. sig. wave height (m)	11.79	14.81	9.91	8.38	5.45	9.91	5.43	5.07	13.42	7.46	9.16
Low. sig. wave height (m)	0.30	0.20	0.10	0.02	0.10	0.20	0.30	0.20	0.01	0.20	0.16
Avg. sig. wave height (m)	1.81	1.73	1.60	1.59	1.59	1.54	1.53	1.57	1.58	1.73	1.63
Highest wave period (s)	11.14	14.80	10.75	11.86	13.69	11.88	11.51	12.79	13.41	13.63	12.55
Lowest wave period (s)	3.47	3.43	3.55	3.30	3.76	3.64	3.41	3.84	3.32	3.81	3.55
Average wave period (s)	5.64	5.94	5.71	5.67	5.90	5.94	5.98	6.14	6.00	6.13	5.91
Avg. wave energy density per unit area of surface waves (J/m^2)	2,016	1,831	1,565	1,552	1,550	1,454	1,435	1,511	1,531	1,838	1,628
Maximum wave energy density per unit area of surface waves (J/m^2)	85,227	134,480	60,214	43,056	18,211	60,214	18,078	15,760	110,422	34,121	57,978

data obtained from NOAA to be used in the analysis (approximately 30.6%). Details about the buoys' depth and location were also recorded as shown on Table 1 and average values across the region on a yearly basis were recorded on Table 2. From this information, the various significant wave heights, wave periods, wave power, and wave energy density values required for a regional WEC were calculated (Table 3).

The dataset obtained, was represented graphically to identify any particular trends or outliers in the population. When this was conducted, the periods of increased significant wave heights and extreme values became apparent in the spread of the annual significant wave height across the region (i.e. the 10 selected buoys) from 2009 to 2018. These extreme values represent storm events that occurred during the year and is utilised via the Peak Over Threshold (POT) method to predict the future 50-year and 100-year return waves via extreme wave analyses [5]. The distributions used for these extreme analyses are the Exponential, Fisher-Tippet, Gompertz, Gumbel, Rayleigh and Weibull [17, 18]. A probability plot was created with the Reduced Variate against the Wave Parameters. The resulting mathematical equation was used to give an approximated prediction at the 50-year and 100-year return period. It is recommended by Penalba, et al. [19] that at minimum 30 years of historical data be used for reliable predictions. Unfortunately, this span of data was not available for the public by NOAA. To circumnavigate this, statistical analyses were employed.

According to NOAA Atlantic Oceanographic and Meterological Laboratory [20], the average number of named storms per year (i.e. Tropical Storms, Hurricanes and Subtropical Storms) in the Atlantic region is 12; this is based on empirical data captured from 1968 to 2015. The highest amount of storms and hurricanes ever recorded in a single year in the Atlantic region since 1930 is 28 and 15 respectively. This energy intensive activity took place in the year 2005. For the purposes of using the distributions in extreme wave analysis of storm events, threshold values will be set to attain 12 assumingly independent peak storms per year from the annual wave spread, in alignment with the average amount experienced annually as stated by [20].

Using the independent 12 peak values per year, the respective significant wave height threshold values were 3.75 m for 2009, 4.00 m for 2010, 4.00 m for 2011, 4.00 m for 2012, 3.75 m for 2013, 4.00 m for 2014, 4.00 m for 2015, 4.00 m for 2016, 6.00 m for 2017 and 4.00 m for 2018. These 12 values over 10

TABLE 3 Proposed design specifications for WECs

Design operating specifications	
Average significant wave height (m)	1.62 ± 1.31 (95% confidence)
Average wave period or energy period (s)	5.91 ± 2.03 (95% confidence)
Average wave speed (m/s)	9.23
Maximum wave speed (m/s)	12.40
Average wavelength (m)	54.53
Maximum wavelength (m)	98.43
Average wave power per unit of wave crest length (kW/m)	7.421
Average wave energy density per unit of surface waves (J/m^2)	1,609.09
Maximum wave power per unit of wave crest length (kW/m)	32.568
Maximum wave energy density per unit of surface waves (J/m^2)	5,256.43
Overall spectral width	0.172
Overall directionality coefficient	0.74
Overall Direction of the maximum directionally resolved wave power (with respect to North)	42°
Extreme wave (100-year return)	19.00 ± 2.78 (95% confidence)
Extreme wave (50-year return)	17.88 ± 2.32 (95% confidence)
Extreme wave climate model	Rayleigh distribution

years, accumulated to the 120-value dataset that would be used for the extreme wave analysis in this study. The 120-value data set contained significant wave heights ranging from 3.75 m to 14.81 m. After attaining the various extreme predicted significant wave heights for the 50-year and 100-year return waves, further statistical analyses (method of least squares) are utilised to identify which distribution best represented the dataset and as such, the wave climate examined. An average of the predicted extreme values from the various distributions was determined and recorded with 95 % confidence. Following this, the probability of failure was calculated for each return period to establish an acceptable design life.

Trends on the wave energy density over the years were plotted graphically and analysed accordingly. This also used statistical analyses such as the Mann–Kendall standard normal test statistic and the Theil-Sen method to determine the projection of the wave energy environment in the future. The different buoys (or locations) were compared to highlight geographical factors associated. Further to this, the significant wave heights and associated wave periods and power were plotted in a scatter form to examine characteristic shapes or relationships.

Following this and utilising the standard IEC [12], the overall spectral width, directionality coefficient and the direction of the maximum directionally resolved wave power were found. It was determined for each individual location positioned by the buoys and then an overall average value was determined. This overall value would be used as the metric to represent the environment on the Atlantic side of the Caribbean.

3 | THEORY/CALCULATION

3.1 | Wave power

Calculations were conducted with the assumption that the Airy Wave Theory applies. Hence, for deep water, the wave energy flux is Wave energy flux per unit of wave-crest length (W/m) as given by the equation:

$$P = \frac{1}{64\pi}\rho g^2 H^2 T, \quad (1)$$

where H is the significant wave height, T is the wave energy period, ρ the sea water density (1000 kg/m^3) and g the acceleration by gravity (9.81 m/s^2) [21].

3.2 | Wave energy density

In a sea state, the average energy density per unit area of gravity waves on the water surface can be calculated from the equation:

$$E = \frac{1}{16}\rho g H^2, \quad (2)$$

where E is the mean wave energy density (kinetic and potential energy) per unit horizontal area (J/m^2) [21].

3.3 | Extreme wave analyses

Using the principles of extreme value analysis, various probability distributions were utilised to represent the ocean wave characteristics. Since each probability distribution theorem gives a different answer, for a better approximation of the extreme significant wave height of a 1 in 50 year return wave and a 1 in 100 year return wave, an average of the Exponential, Fisher Tippet, Gompertz, Gumbel, Rayleigh and Weibull distributions was used. See World Meteorological Organisation Secretariat [17] and BSI [18] for more details regarding their use, the formulas employed and how to extrapolate the data.

3.4 | Peak over threshold (POT) method

This methodology is used for acquiring the dataset for extreme wave analyses. It is assumed that the storm events are independent of each other, for the POT method to be used for sampling. The POT method considers local maxima or peaks due to storms above a determined threshold. [6]

3.5 | Long-term wave analysis

The data points utilized in long-term wave analysis and prediction must be independent of each other. This analysis of

long-term wave statistics involves the study of statistical properties of wave over a significant amount of time. In comparison, short-term wave parameters are considered constant due to the short timeframe under evaluation. For short-term data, the average hourly height will be influenced by the average wave height from the previous hour. Hence, theoretically, short-term data condition cannot meet the requirements unless storm events alone are considered for the POT [5]. Also, with long term wave analysis, a greater understanding of wave behaviour can be obtained as it takes into account factors such as seasonal or yearly variations, changes in the climate globally and other sea conditions that would affect results [22].

3.6 | Probability of the return period

$$P_{nx} = \frac{T_0}{T_r}\left(\frac{1}{n_x + 1}\right), \tag{3}$$

where P_{nx} is the probability of the event associated with the return period T_r, n_x is the number of data points in the time T_0 (years). The return period is an average time or an estimated average time between extreme events [18].

3.7 | Z score

Since it is unknown, which probability distribution is the most suited, an average of the five was calculated and the Z Score for each found using the formula [23]:

$$Z = \frac{x - \mu}{\sigma} \tag{4}$$

3.8 | 95% Confidence interval

When the standard deviation is known, the limits for the values with 95% confidence are:

$$\text{Lower limit} = \mu - Z\left(\frac{\sigma}{\sqrt{n}}\right), \tag{5}$$

$$\text{Lower limit} = \mu + Z\left(\frac{\sigma}{\sqrt{n}}\right), \tag{6}$$

where x is the extreme value obtained from the distribution, μ is the mean of the distributions being analysed, σ is the standard deviation of the distributions being analysed, Z is the amount of standard deviations from the mean and n is the sample size (the number of distributions used). Z for 95% confidence is equivalent to 1.96 [23].

3.9 | Coefficient of determination

To assess how linear regression models fit the data set, the coefficient of determination (R^2) is used. The formula used is as follows:

$$\text{Coefficient of determination}\left(R^2\right) = \frac{SS_R}{SS_T}, \tag{7}$$

$$SS_R = \sum_{i=1}^{n}\left(\hat{y}_i - \bar{y}_i\right)^2, \tag{8}$$

$$SS_T = \sum_{i=1}^{n}\left(\hat{y}_i - \bar{y}_i\right)^2 + \sum_{i=1}^{n}\left(y_i - \hat{y}_i\right)^2, \tag{9}$$

where $0 \le R^2 \le 1$ and the closer R^2 is to 1 the better the model represents the data set. SS_R is the regression sum of squares, that is the variability due to the regression model and SS_T is the total sum of squares. It is a measure of total variability, which includes the variability due to the regression line and error. [23].

The Mann–Kendall standard normal test statistic is used to determine the monotonic incline or decline of a trend. It is used extensively in hydro-meteorological time studies. More details concerning the use of the method can be found at Gocic and Trajkovic [24].

Sen's slope estimator is a non-parametric method for estimating the slope of a trend examined. This methodology is employed when the dataset does not fit a straight line, thus invalidating the estimations made from a regression line using the least squares concept. Its insensitivity to outliers is what makes it relevant. More details concerning the use of the method can be found at Gocic and Trajkovic [24]. It was first published by Sen in 1968.

3.10 | Failure probability

$$\text{Probability of exceedance (\%)} = 100 \times \left(1 - \left(1 - \frac{1}{T}\right)^N\right), \tag{10}$$

where T is the return period and N is the design life in years. This value calculated represents the probability that the T year event will occur in the next N years. [18]

3.11 | Spectral width

$$\epsilon_0 = \sqrt{\frac{\sum_i \overline{J_{i,j}} \sum_i \left[\overline{J_{i,j}} f_i^{-2}\right]}{\left\{\sum_i \left[\overline{J_{i,j}} f_i^{-1}\right]\right\}^2} - 1}, \tag{11}$$

where i is the index representing discrete frequency, j is the index representing discrete direction, $\in_0$ as the spectral width, f_i is the frequency (Hz) and $\overline{J_{i,j}}$ is the mean wave power spectrum (W/m). The equation expressed is adapted from Ahn and Neary [25] and the IEC [12]. According to the IEC [12], the spectral width "characterizes the relative spreading of energy along the wave spectrum" and is defined as "the standard deviation of the period variance density, normalized by the energy period". For interpretation purposes, the smaller the value obtained, the narrower the frequency bandwidth exhibited.

3.12 | Directionally resolved wave power

$$\overline{J_i}\ (\alpha) = \sum_j \overline{J_{i,j}} \cos(\alpha - \theta)\,\delta, \tag{12}$$

$$\delta = 1, \text{when } \cos(\alpha - \theta) \geq 0,$$

$$\delta = 0, \text{when } \cos(\alpha - \theta) < 0,$$

where i is the index representing discrete frequency, j is the index representing discrete direction, $\overline{J_i}(\alpha)$ is the directionality resolved wave power (W/m), $\overline{J_{i,j}}$ is the omnidirectional wave power (W/m) and α is the angle (in degrees) of the directionally resolved wave power. α has a resolution of 1° and it is taken clockwise from true North (0° to 360°). This equation expressed is adapted from Ahn and Neary [25] and the IEC [12]. According to the IEC [12], the maximum directionally resolved wave power is "the maximum time averaged wave power propagating in a single direction".

3.13 | Direction of maximum directionally resolved wave power

The associated angle α for the maximum directionally resolved wave power identified is the direction of maximum directionally resolved wave power [12].

3.14 | Directionality coefficient

$$d_{\overline{J_i}} = \frac{\max\left[\overline{J_i}(\alpha)\right]}{\overline{J_i}}, \tag{13}$$

where $d_{\overline{J_i}}$ as the directionality coefficient, $\max[\overline{J_i}(\alpha)]$ is the maximum directionally resolved wave power identified (W/m) and $\overline{J_i}$ is the corresponding total wave power (W/m). This equation is adapted from Ahn and Neary [25] and the IEC [12]. According to the IEC [12], the directionality coefficient is "a characteristic measure of the directional spreading of wave power". A small value is interpreted as the wave energy resource displaying wide directional spreading.

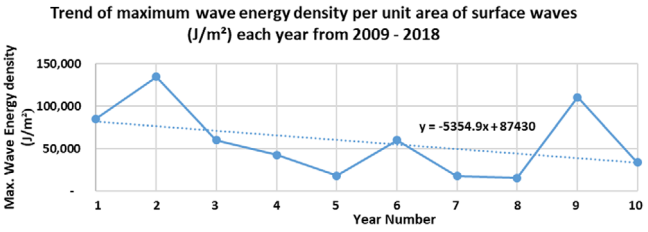

FIGURE 2 Trend of maximum wave energy density per unit area of surface waves throughout the years

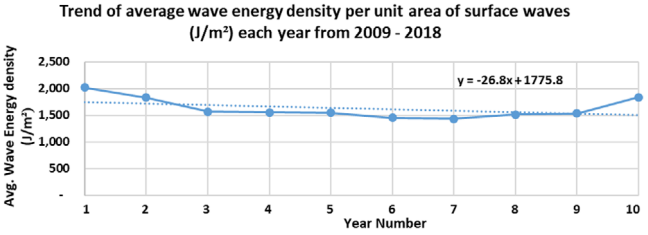

FIGURE 3 Trend of average wave energy density per unit area of surface waves throughout the years

4 | RESULTS

In the analysis of this study showed in Figure 2, the maximum wave energy density per unit area of surface waves in the region has been on the decline as reflected by the linear regression line illustrated. The Mann–Kendall standard normal test statistic (Z_S) calculated is −1.62 and the Sen's slope estimator (Q_{MED}) found for Figure 2 was determined to be −18.8 (within an interval of −93.8 and 19.3 for 95% confidence).

The analysis of this study showed in Figure 3 the linear regression line that the variation in the average wave energy density per unit area of surface waves in the region was on a decline, though minimal. Over the 10 years observed, the average wave energy experienced fluctuated between 1500 J/m^2 and 2000 J/m^2. The Mann–Kendall standard normal test statistic (Z_S) calculated is −1.53 and the Sen's slope estimator (Q_{MED}) found for Figure 3 was determined to be −6523.1 (within an interval of −18566.7 and 3182 for 95% confidence).

Figures 4 and 5 showed that the area surrounding buoys 41043, 41044 and 41046 experience significantly higher maximum wave energy density per unit surface area than the other locations and are also within the higher range for average wave energy density per unit surface area. The location of buoys 41040 and 41041 have the highest 10-year average wave energy but relatively low 10-year maximum wave energy values when compared with the other sites analysed. The locations of buoys 41052, 41053, 42060 and 42085 have the lowest 10-year average wave energy and low 10-year maximum wave energy consistently.

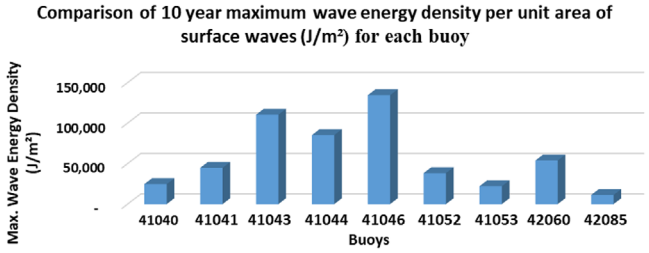

FIGURE 4 Comparison of 10-year maximum wave energy density per unit area of surface waves for each buoy

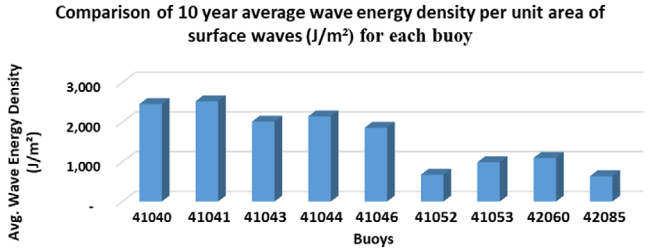

FIGURE 5 Comparison of 10-year average wave energy density per unit area of surface waves for each buoy

On Table 4, we can see the variation of the spectral width, directional co-efficient and direction of maximum directionally resolved wave power across the region and by the different buoys. No value was obtainable for the spectral width of buoys 41052, 41053 and 42085 due to data concerning wave period.

On Figure 6, all the buoys examined had a relatively stable spectral width amongst them, while on Figure 7 all the buoys had relatively high directionality coefficients except 41041, 41052, 42060 and 42085. There were no geographical commonalities found between them, that sets them apart from the rest.

TABLE 4 Spectral width, directionality coefficient and direction of maximum directionally resolved wave power spread throughout the Caribbean

Buoy	Spectral width	Directionality coefficient	Direction of maximum directionally resolved wave power (in degrees clockwise from north)
41040	0.151	0.92	351
41041	0.173	0.38	9
41043	0.187	0.74	42
41044	0.191	0.88	3
41046	0.191	0.84	33
41052	N/A	0.04	275
41053	N/A	0.88	24
42060	0.131	0.55	16
42085	N/A	0.50	60
Overall	0.172	0.74	42

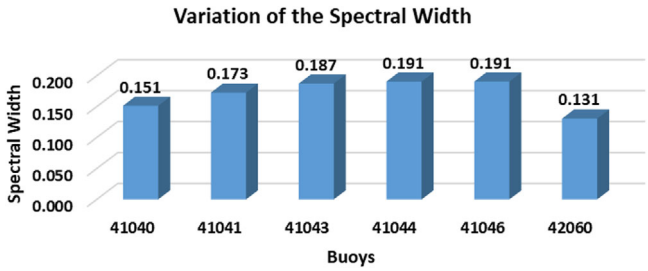

FIGURE 6 Comparison of spectral width across the Caribbean

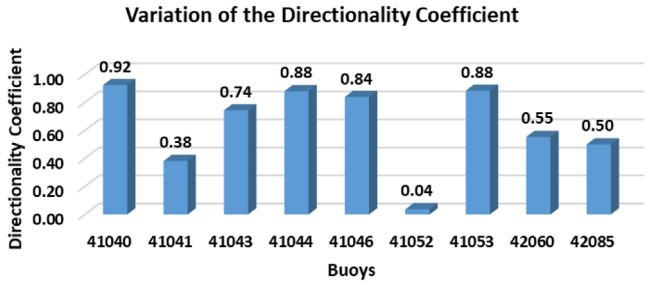

FIGURE 7 Comparison of directionality coefficient across the Caribbean

4.1 | Data spread of the significant wave height, the average wave period and the average wave power

Each buoy except 41052, 41053 and 42085 was individually analysed in Figures 8–13 for correlations between their significant wave height, average wave period and average theoretical wave power based on data obtained over the 10 years. Buoys 41052, 41053 and 42085 were left out of this analysis because their wave data did not provide sufficient information on their respective wave periods. Figure 14 illustrates the correlation across the region for all the buoys in the analysis. The wave spread showed no characteristic trait other than between the average wave power and the significant wave heights. The overall shape of the significant wave height is expected to be reflected on the overall shape of the average wave power. This is because it is mathematically directly proportional to each other.

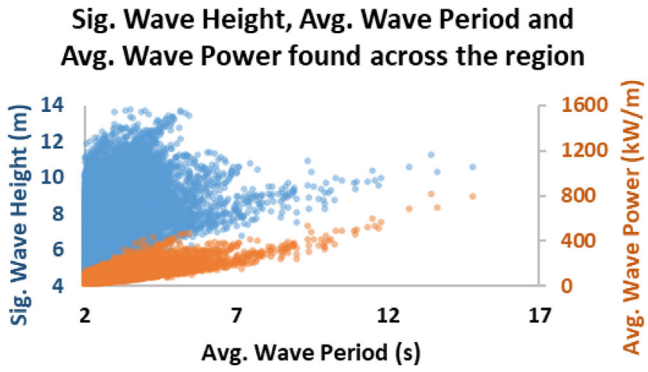

FIGURE 8 Significant wave height, the average wave period and average wave power found across the region

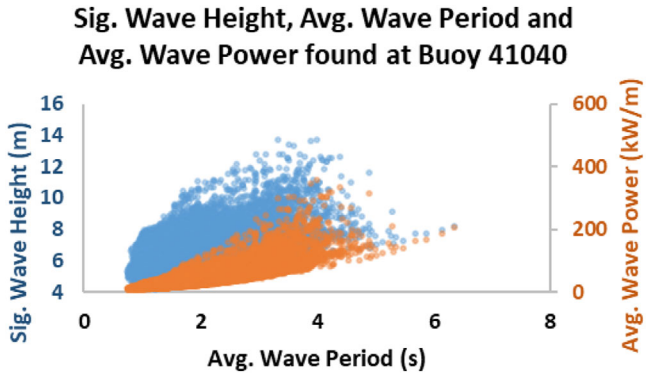

FIGURE 9 Significant wave height, the average wave period and average wave power found at buoy 41040

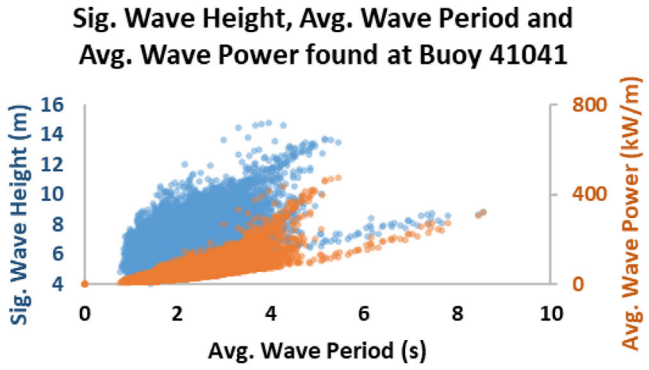

FIGURE 10 Significant wave height, the average wave period and average wave power found at buoy 41041

4.2 | Percentage occurrence of the significant wave height, average wave period and average wave power

The percentage occurrence shown on Figure 15 indicates that all the buoys on average maintain approximately 55–75% of their dataset in the region of 1–2 m.

The percentage occurrence shown in Figure 16 indicates that all the buoys on average maintain approximately 45–60% of

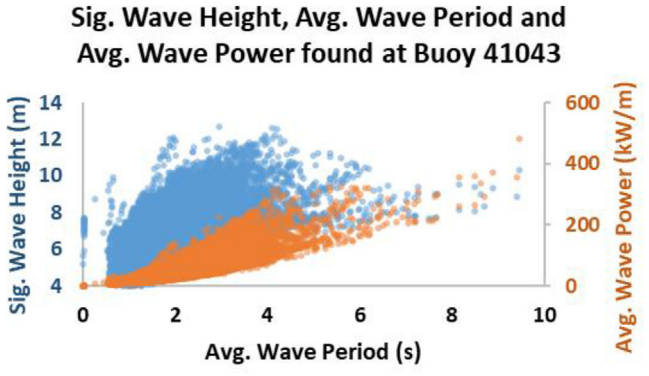

FIGURE 11 Significant wave height, the average wave period and average wave power found at buoy 41043

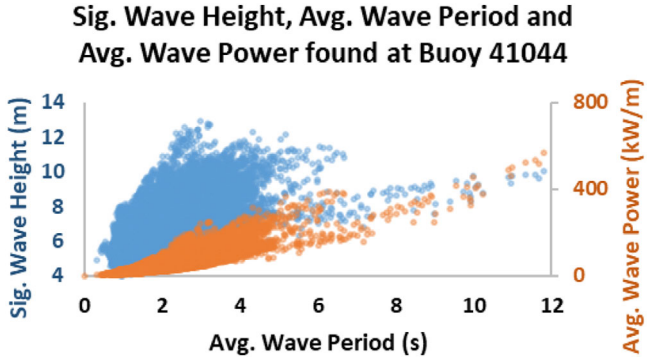

FIGURE 12 Significant wave height, the average wave period and average wave power found at buoy 41044

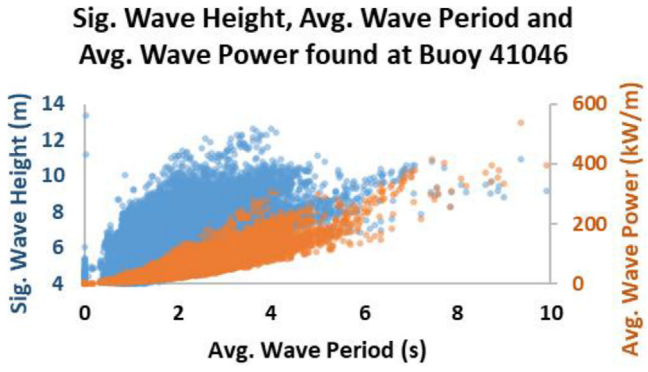

FIGURE 13 Significant wave height, the average wave period and average wave power found at buoy 41046

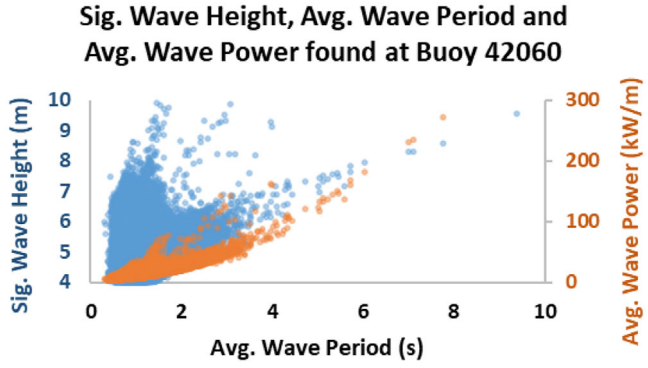

FIGURE 14 Significant wave height, the average wave period and average wave power found at buoy 42060

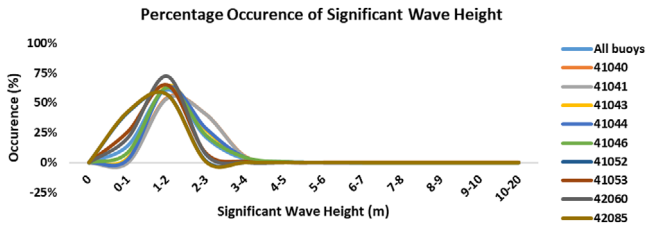

FIGURE 15 Percentage occurrence of the significant wave height

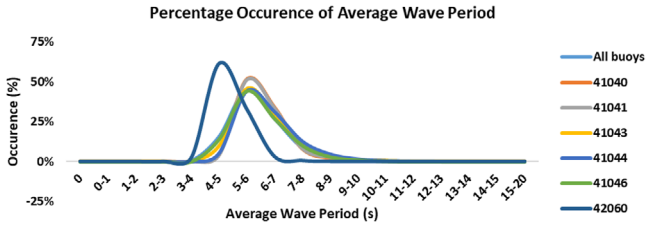

FIGURE 16 Percentage occurrence of the average wave period

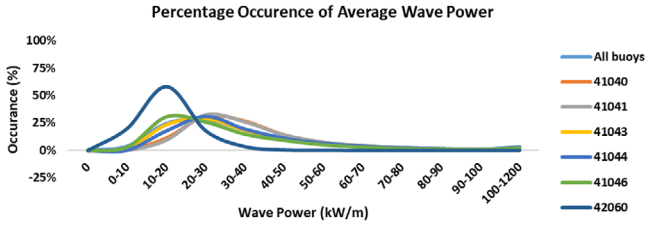

FIGURE 17 Percentage occurrence of the average wave power

their dataset in the region of 4–7 s. Majority, however, appear to be concentrated between 5 and 7 s.

The percentage occurrence shown in Figure 17 indicates that the wave power is less uniformed than the average significant wave height and wave period. The spread of the values are a lot more pronounced.

4.3 | Extreme value analyses

According to the Exponential distribution, for a return period of 100 years and 50 years, the extreme significant wave heights is 21.7 m and 20.0 m, respectively. These values were obtained using the equation of the line:

$$y = 2.4667x + 4.2265. \quad (14)$$

According to the Fisher Tippet distribution, for a return period of 100 years and 50 years, the extreme significant wave heights are 14.4 m and 14.3 m respectively. These values were obtained by using the equation of the line:

$$y = 0.4942x - 2.5277. \quad (15)$$

According to the Gompertz distribution, for a return period of 100 years and 50 years, the extreme significant wave heights are 15.5 m and 15.0 m, respectively. These values were obtained by using the equation of the line:

$$y = 4.5538x + 6.5784. \quad (16)$$

According to the Gumbel distribution, for a return period of 100 years and 50 years, the extreme significant wave heights are 21.0 m and 19.4 m, respectively. These values were obtained by using the equation of the line:

$$y = 2.2687x + 4.8919. \quad (17)$$

According to the Rayleigh distribution, for a return period of 100 years and 50 years, the extreme significant wave heights are 18.3 m and 17.4 m, respectively. These values were obtained by using the equation of the line:

$$y = 0.5221x + 1.8858. \quad (18)$$

According to the Weibull distribution, for a return period of 100 years and 50 years, the extreme significant wave heights are 23.0 m and 21.1 m, respectively. These values were obtained by using the equation of the line:

$$y = 0.9829x + 1.0291. \quad (19)$$

From the table we can identify that the Rayleigh distribution has the lowest Z score for both the 50-year and 100-year return wave. Its coefficient of determination was also the largest at 0.9968. This means that 99.68% of the dataset used for the extreme value analysis fit the Rayleigh distribution.

When analysing the data we can see that the Fisher-Tippet distribution provided the lowest return wave heights and the closest to the largest extreme wave currently known in the data set (14.81 m).

4.4 | Probability of failure

Table 3 presents the calculated data that outlined the proposed design requirements for a regional WEC. It was created with a 95% confidence interval.

5 | DISCUSSION

The data analysed in this study was from nine buoys located across the Caribbean region at varying depths. According to NOAA National Data Buoy Center [14], the accuracy of data recorded for the significant wave height, period and direction was ±0.2 m, ±1 s and ±10°, respectively. NOAA/NDBC utilised spectral hindcast data, modelled from WAVEWATCH III. This particular system was preferred for analyses on the Atlantic Ocean side of this region because it catered for complex sea states developed by swells and localised winds. An analysis based on the JONSWAP spectrum exhibited a slight overestimation when compared to hindcast data and yielded large instant errors due to its focus on unimodal sea states. This focus prevented the model from accurately assessing the spectral distribution of the native energy found in this region [26]. When Campos and Soares [27], compared 3 hindcast models: the ERA-Interim, NOAA (based on WAVEWATCH III) and HIPOCAS (based on the REMO wind model), they found that at non-extreme conditions the hindcasts were effectively

equivalent as their biases for significant wave height was less than 0.5 m. However, when comparing wind and wave errors, WAVEWATCH III was the best model for accuracy and was suggested to be the model of choice for latitudes below 30° North (as is the case in this study).

Data showed the contribution of localised wind energy and swell energy were particular phenomenon that can affect the wave energy climate in regions located at significant distances from its source. Munk, et al. [28] found that swells could propagate to distances up to one-half of the Earth's perimeter, leading to mixed energy climates and provided a sound basis why accurate resource analyses should be built on hindcast data. A study conducted by Zheng, et al. [29], illustrated that the source of swell energy in a particular area changed throughout the year. As such, the impact on Caribbean region wave energy is influenced by various distant regions globally.

The trend of the maximum wave energy experienced on Figure 2 indicated that the extreme levels have been reducing regionally over the years. The downward monotonic trend is seen via the regression line illustrated on the Figure 2. This was confirmed by the negative Mann–Kendall test statistic (Z_S) and the Sen's slope estimator (Q_{MED}) calculated. It is uncertain as to when this trend started since the data analysed in this study was only from the year 2009. One can assume that this will work in favour of device survivability due to reduced cyclic loading of high-energy waves, as this is a stated major challenge faced by the community to date by multiple sources including Mofor, Goldsmith and Jones [30]. It will also facilitate appropriate scheduled maintenance activities, as devices will be more accessible due to "safer" climate conditions [31]. This can also increase the device's design life and improve sustainability.

In addition to the maximum wave energy being on a decline, the average wave energy experienced is also on a decline, as it fluctuated between 1500 J/m^2 and 2000 J/m^2 (Figure 3). Similarly, the downward monotonic trend was seen via the regression line on Figure 3. This was confirmed by the negative Mann–Kendall test statistic (Z_S) and the Sen's slope estimator (Q_{MED}) calculated. Therefore, WECs designed for the Caribbean region should be focused on optimizing operating conditions within this range. This narrow range presents an opportunity and is a critical finding of the study. It lays the groundwork for devices to be developed that will have a relatively high percentage utilisation value. That is, devices should be able to employ a significantly large amount of time undergoing productive energy harvesting operations as opposed to retracting into survival mode when waves are too large or at standstill when waves are too small. This translates to increased sustainability and greater return on investment. Guanche, et al. [31] expressed this concept as device availability.

The mathematical equations in Figures 2 and 3 could be utilised for predicting the maximum or the average wave energy in the region, thus facilitating better planning practices for project developers. A longer timeline would have given the analysis more rigour; however, that data was not accessible as wave-measuring devices are highly unreliable due to the harsh ocean environment. Comparison of these trends found would have been useful for academic purposes, but unfortunately, it was not identified in literature. Only a snapshot in time on energy potential was found [32, 33]. Mann–Kendall Test and Theil-Sen method utilised their non-parametric nature to confirm the decline presented by the regression lines. These methods were considered more applicable, as the data set was not naturally linear and it takes into account how outliers can skew the regression trend lines. It was built on the median of the slopes of all lines passing through pairs of points in the data set.

In the analysis in Figures 4 and 5, the commonalities found for buoys 41043, 41044 and 41046 were their geographic locations (Table 1). This may explain why they possessed a significantly higher maximum wave energy density per unit surface area and was in the higher range for average wave energy density per unit surface area. These three buoys are located between 20° and 30° North latitude. This finding is in line with the work of Waters [32] and Arinaga and Cheung [33], which showed that the closer you were to 30° north latitude in the Caribbean region, the greater the wave energy was expected to be. As such, it is confirmed that these locations will experience greater extreme events and will release vicious forces on devices located there. This expected action will inevitably decrease the survivability potential at those sites. Therefore, it is suggested that larger devices or devices with high material strength would be most applicable at those locations. Alternatively, the sites of buoys 41040 and 41041, which possessed the highest 10 year average wave energy with relatively low 10 year maximum wave energy values seemed better suited for clusters of medium sized devices in large groups. Also, the locations of buoys 41052, 41053, 42060 and 42085 were considered prime candidates for micro WECs as they have the lowest 10-year average wave energy values and low 10-year maximum wave energy. These micro WECs, would not have to be as robust as other sites, but should be developed in a large farm like arrangement for sufficient energy harvesting. However, the creation of site-specific devices was not the thesis of this study, but really that of the criteria for a regional WEC.

The results of this study showed that a regional WEC should be designed with the capability of absorbing energy from waves with heights ranging from 0.3 m to 2.9 m, with the optimal working range between 1.0 m and 2.3 m (i.e. the average significant wave height ± 1 standard deviation). A device operating in this range should capture approximately 68% of the waves passing, assuming a normal distribution. Additional metrics include wave periods (or energy periods) ranging from 3.9 s to 7.9 s, and wave speeds around 9.2 m/s. It was found that devices in this region have the potential to absorb theoretically 7.4 kW/m of average wave power and 1,609 J/m^2 of average wave energy density.

The average wave power of 7.4 kW/m determined in this study for the general region, is analogous with the 5–10 kW/m range reported by Ahn and Neary [9] around Puerto Rico (located in the Caribbean region). The maximum wave energy flux per unit of wave crest length is equivalent to 32.568 kW/m and the maximum wave energy density per unit area of surface waves is equivalent to 5256 J/m^2. These energy values are theoretical and do not take into consideration losses due to friction, noise, etcetera. The buoys that were used for this study

were located in a region with an average depth of 2924 m. (See Table 1 for actual details regarding water depth at each buoy location).

Additional metrics to be used in a regional WEC design include overall spectral width of 0.172, overall directionality coefficient of 0.74 and the overall direction of the maximum directionally resolved wave power (with respect to North) as 42°. This information coincided with Ahn, Haas and Neary [8], who determined the directionality coefficients by the Gulf of Mexico (eastern coast) and the Florida Channel to be 0.78 and 0.77, respectively. They also identified that Puerto Rico had a directionality coefficient of 0.89, which was comparable to the 0.88 value found at buoy 41053 (located just north of Puerto Rico) in this study (Table 4). It is clear that the concept of an overall directionality coefficient for a regional device has some merit but there requires a tolerance that must be implemented. A directionality coefficient of 0.74 means that the energy supply expresses generally a narrow range in directional spreading. As such, the maximum wave energy is propagated from a singular direction on average. This works well with WECs that take some time to realign its energy absorption mechanism, ensuring operational efficiency due to direction. An example of this in use may be the Wave Overtopping technology, demonstrated by the Wave Dragon. A high directionality coefficient is a welcomed advantage for WECs, as devices would experience a more focused energy supply with little need for realignment. However, buoys 41041, 41052, 42060 and 42085 seemed to experience a wide range in directional spreading of the wave energy. Further investigation should be performed to explain this finding.

Ahn, Haas and Neary [8] determined that the Gulf of Mexico (eastern coast), the Florida Channel and Puerto Rico have spectral widths of 0.3, 0.27 and 0.27, respectively. It is not particularly comparable to the overall spectral width found in this study, and may be a result of the location of the buoys. The best suited buoy for comparison with Ahn, Haas and Neary [8] would have been buoy 41053, located near Puerto Rico. Unfortunately, sufficient data was not found for buoys 41052, 41053 and 42085 to determine the locations's spectral width. As such, this information was not presented in Table 4 nor was it taken into consideration for the overall spectral width calculated. It can be reasonably stated that since the overall spectral width in this study was smaller than what was found in the Gulf of Mexico and inside the Florida channel by Ahn, Haas and Neary [8], the Atlantic side of the Caribbean yields a narrower frequency bandwidth. Small spectral widths is optimal for WECs that have, like the point absorbers (e.g. Powerbuoy and Wavestar), submerged pressure differential devices (e.g. Archimedes Wave Swing) and attenuators (e.g. the Pelamis) because they allow developers to match the device frequency from bobbing with the natural frequency of the wave environment. This in turn makes the devices operate more optimally, as it improves the energy captured by the absorption mechanism once they are synchronised with their surroundings. As all the buoys presented on Figure 6 had a relatively stable spectral width amongst them, the overall value is a reasonable representation of the individual locations.

Since the direction of maximum directionally resolved wave power was identified to be 42° clockwise from true North, developers now know how to align fixed WECs for maximum energy capture. Technologies like the Oscillating Wave Surge concept (demonstrated by the Aquamarine Power Oyster), the Oscillating Water Column principle positioned on coastlines (e.g. Wavegen Limpet) and those that are coupled to coastal protection systems (e.g. the SeaWave Slot-Cone Generator) should be positioned perpendicularly to this 42° angle for optimal operation and improved efficiency. This is paramount as these technologies cannot reposition their orientation automatically depending on the principal wave direction. A perpendicular direction to the 42° angle would reduce the energy loss as more of the energy absorption mechanism is engaged.

Figures 8–13, identified the average wave periods with the highest loads (i.e. significant wave height) experienced. Developers could use this graphical display for their design calculations of marine energy converters. The illustration of this historical data spread can assist in identifying exactly where on the performance scale to locate the devices. From observation, Figures 8–13 showed no clear relationship between the average significant wave height and the average wave period. However, according to IEC [13], the wave period T, in combination with the normal wave height follows the relationship:

$$11.1\sqrt{\frac{H_{S,NSS}(V)}{g}} \leq T \leq 14.3\sqrt{\frac{H_{S,NSS}(V)}{g}}, \qquad (20)$$

where $H_{S,NSS}$ is the significant wave height of the normal sea state (m), V is the 10-minute mean wind speed (m/s) and T is the wave period (s) [13]. Contours could be added to the scatter diagram on Figures 8–13 and used to identify the one-dimensional design load criteria for WEC. Coe, Yu and van Rij [34] illustrated this concept well via their review of specific researchers. They also expressed the need for a correction factor to be applied so that bias was reduced in the calculation process. When using the contour lines to predict a response, it was recommended that developers use the largest response as the baseline for their design criteria on wave energy converters (for more information around this topic, see Coe, Yu and van Rij [34]).

Figures 15–17 represent the percentage occurrence of the average significant wave height, wave period and wave power. The representation takes the form of a normal distribution as expected based on the size of the dataset. The general peak of the normal distribution graphs revolved around the calculated average significant wave height and wave period of 1.62 m and 5.91s, respectively. However, Figure 17 has a less steep normal distribution as the theoretical wave power for the different locations (or buoys). It should be noted that the missing buoys (41052, 41053 and 42085) would have skewed Figure 17 negatively, as those buoys are located in a very unenergetic region of the Caribbean with low significant wave heights. As identified on Table 1, the depth at their location is between 17 and 44 m. This indicates that the buoy could be considered near shore and as such due to shoaling and other oceanographic processes,

TABLE 5 Calculation of the range required for 95% confidence in capturing the extreme significant wave heights

Calculation for range with 95% confidence		
	100-year return	**50-year return**
Sample size	6	6
Standard error (mean)	1.423	1.137
Level of confidence, $1 - \alpha$	95.0%	95.0%
Significance level, α	5.0%	5.0%
$\alpha/2$	2.5%	2.5%
From normal distribution tables, $Z_{\alpha/2}$	1.96	1.96
Lower limit	16.21	15.56
Upper limit	21.78	20.11

their energy would have already begun dissipating. These figures allow designers to create optimized WECs that fit their normal distribution profile and extend their ability to capture the energy of a large percentage of the expected environment.

The POT method was used to determine the extreme wave climate possible with the number of peaks per year as 12. As different years had different experiences, the threshold levels utilised varied and so did the extreme values used. For the years 2009 and 2010, the peaks (or extreme waves) were found between the months of May and August, while for the other years it began around the month of June and intensified towards November/December. This coincided with the violent winds brought by the region's annual hurricane season. Different researchers utilised different methods to obtain the POT, including the use of the data found above a percentile value (e.g. top 0.5%) dictated by a Poisson process, as is the case in Caires and Sterl [35] or the use of observed maximas demonstrated by Alves (2004) [36]. The use of adjustable thresholds for this study was considered more practical as we know from historical data the average expected number of storm events in the region.

Extreme value analysis with 95% confidence showed waves with heights from 16.2 m to 21.8 m for a 1 in 100 year return wave if the significance level (α) were 5% (see Table 5). The average significant wave heights for a 1 in 100 year return wave was 19.0 m. This was determined after analysing the data obtained from the buoys over a 10-year period with the Exponential, Fisher-Tippet, Gompertz, Gumbel, Rayleigh and Weibull PDFs. The probability plots are shown graphically in Figures 18–23. The Method of Least Squares was used to generate a best-fit line to determine the extreme significant wave heights at specific return periods via their respective mathematical equations.

Using the Exponential, Fisher-Tippet, Gompertz, Gumbel, Rayleigh and Weibull distributions, significant wave heights of 21.7 m, 14.4 m, 15.5 m, 21.0 m, 18.3 m and 23.0 m were obtained, respectively, for a 1 in 100 year return wave. Mathiesen, et al. [6], articulates the procedure followed for extreme wave analysis. In that study, the three-parameter Weibull distri-

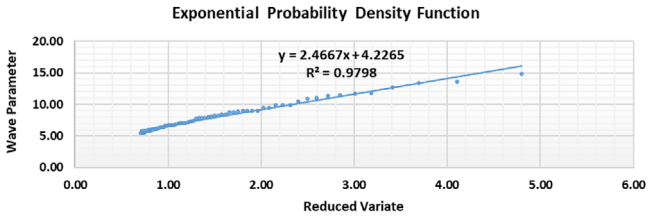

FIGURE 18 Extreme value analysis using the exponential PDF

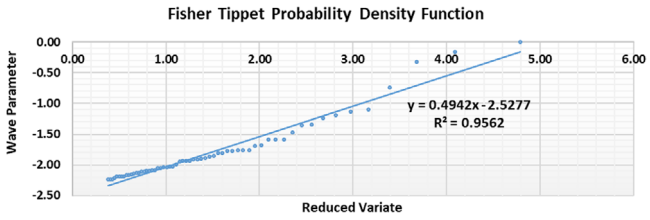

FIGURE 19 Extreme value analysis using the Fisher Tippet PDF

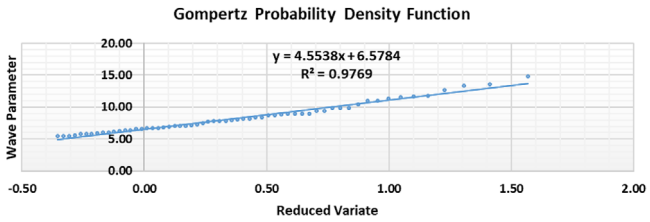

FIGURE 20 Extreme value analysis using the Gompertz PDF

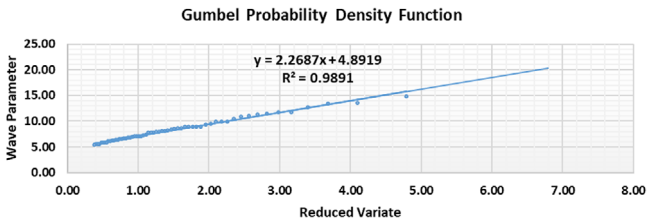

FIGURE 21 Extreme value analysis using the Gumbel PDF

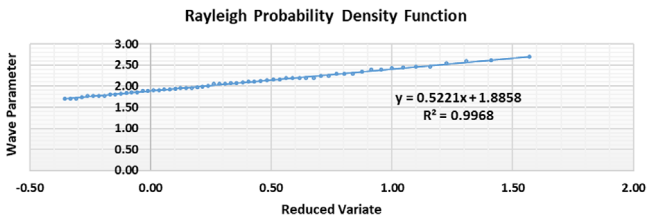

FIGURE 22 Extreme value analysis using the Rayleigh PDF

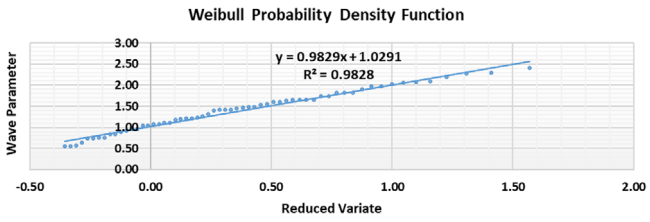

FIGURE 23 Extreme value analysis using the Weibull PDF

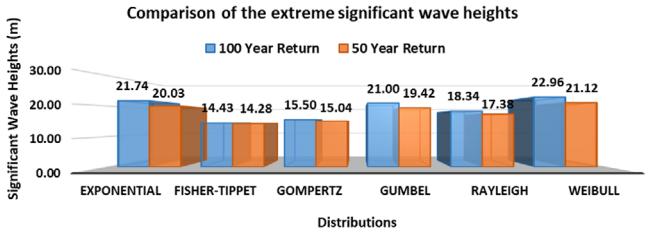

FIGURE 24 Comparison of extreme significant wave heights based on various PDFs

TABLE 6 Summary of the extreme values from the six probability distributions utilised

	Extreme significant wave height (m)		Z Score		
Probability distribution	**100 year return**	**50 year return**	**100 year return**	**50 year return**	**R^2 value**
Exponential	21.74	20.03	0.79	0.77	0.9798
Fisher Tippet	14.43	14.28	1.31	1.29	0.9562
Gompertz	15.50	15.04	1.00	1.02	0.9769
Gumbel	21.00	19.42	0.58	0.55	0.9891
Rayleigh	18.34	17.38	0.19	0.18	0.9968
Weibull	22.96	21.12	1.14	1.16	0.9828
Average, μ	19.00	17.88	0.83	0.83	0.9803
Std. deviation, σ	3.49	2.78	0.41	0.42	0.0138

bution was assumed to be the most acceptable for ocean wave analysis. However, it does not limit the use of other distributions. Since it is unknown, which distribution may be the most applicable for ocean waves in the Caribbean region, the average of the six distribution models was used to minimise the risk of erroneous results. The analysis indicated that to protect the investment, WECs in the Caribbean region should be designed to withstand the forces associated with a significant wave height of 21.8 m (upper end, 95% confidence).

If one distribution had to be chosen to predict the wave environment encountered by these buoys, it would be the Rayleigh distribution. This is because it had the smallest Z scores (0.19 for the 100-year return event and 0.18 for the 50-year return event) when compared against the mean of the extreme significant wave height calculated from the six distributions (Table 6). This indicated that the significant wave heights determined via the Rayleigh distribution were ± 0.19 and ± 0.18 standard deviations from the mean values, respectively. Additionally, the trend line generated when the Rayleigh distribution was used fit the dataset the best (Figure 22). It had a coefficient of determination (R^2) value of 0.9968 (meaning the regression line fit approximately 99.7% of the dataset adequately), which is the highest of all the distributions. Second to the Rayleigh distribution in both the Z scores calculated and the coefficient of determination, was the Gumbel distribution. These results indicate that the conclusions made by Mathiesen, et al. [6], that "the three-parameter Weibull distribution provides an acceptable fit for wave heights in most oceans" and the preference by

TABLE 7 Failure probability (1 in 100 year event)

Design life (years)	Probability of exceedance (%)
1	1.00%
10	9.56%
25	22.22%
30	26.03%
50	39.50%
75	52.94%
100	63.40%

TABLE 8 Failure probability (1 in 50 year event)

Design life (years)	Probability of exceedance (%)
1	2.00%
10	18.29%
25	39.65%
30	45.45%
50	63.58%
75	78.02%
100	86.74%

Muzathik, et al. [5] for the Gumbel distribution are valid, but the Rayleigh distribution is more accurate in the Caribbean context. Potential reasons for the variation amongst the extreme wave heights found by the distributions include the wide range of the data set used (3.75 m to 14.81 m), the timeline of 10 years (30+ years would have been more appropriate), and the use of various site locations as opposed to a singular one.

According to the European Marine Energy Centre [37], the recommended notional design life for a marine energy system is between 10 and 30 years. As shown in Tables 7 and 8, when a 30-year design life is considered, the probability of a 1 in 100-year event will be approximately 26%. While the probability for a 1 in 50-year event will be approximately 45.5% for the same design life. The design life is ultimately the minimum timeframe required for a return on the investment. As such, the design life will be based on the design basis and the financial requirements of the project. Some measure of calculated risk may be required to determine what is considered acceptable. However, the better recommendation is that a design life of 30 years be used and the WEC be capable to withstand a 1 in 100-year event.

The findings from this study should not be taken in isolation for WECs design. The results should be taken in context and serve as information for the academic and research communities to use towards the advancement of this industry. Additional information that should be examined for a complete design of a WEC at a proposed location according to European Marine Energy Centre [37] includes:

- Bathymetry or coastal topography.
- Seabed structure.

- Wind loading, humidity and air temperature for devices protruding in the air.
- Water salinity, temperature and silt content.
- Tidal level.
- Combined effects of high tides, storm surges and waves.
- Sea level rise.
- Current velocities from tidal streams, circulation, winds, storm surge and turbulence.
- Wave actions and loading.
- Increase load and damping from marine growth build up on structure.
- Marine life.
- Geotechnical parameters e.g. soil shear strength, seabed conditions, etc.
- Stability of the seabed.
- Seismic activity of the area.

The results in Table 3 present a summary of the optimized working conditions for WECs intended to be used on the Atlantic side of the Caribbean region. Based on the data from nine buoys over 10 years, an understanding of the characteristic traits of the wave energy in the region was obtained. WECs designed on these metrics should have the capability of absorbing energy from a significantly larger amount of the ocean waves encountered.

6 | CONCLUSIONS

The objective of this research was to determine and present key data for the development of WECs in the Caribbean region. In this study, the operational range for a regional WEC was identified. The calculated data was based on historical wave information that was analysed to predict future performance. Additionally, the information is expected to improve the development of wave energy harvesting in the Caribbean region, as it details critical knowledge about design requirements for successful projects. Its main goal is to provide information that will facilitate the development of a WEC, capable of being utilised anywhere on the Atlantic side of the Caribbean region and not one that is site specific. This will:

- Reduce the cost and time of prototype generation;
- Reduce the design costs for devices at different locations utilising the same principle;
- Enable the development of technical standards for WECs in the region; and
- Expedite the ability for devices to be mass manufactured as the economies of scale has increased, thereby reducing individual unit costs.

The analysis methods utilised in this study are well developed but the research is novel, as it has not been extensively practiced in this region for this purpose. Similarly, detailed information like this packaged for different regions (especially SIDS across the world) could accelerate the development of devices and the UN 2030 Agenda for Sustainable Development. The key findings of the study showed, that for a WEC to be regional in the Caribbean it should facilitate the following:

- Average significant wave heights of 1.62 m.
- Average wave period of 5.91 s.
- Average wave speed of 9.23 m/s.
- Average wave energy flux of 7.421 kW/m of wave crest.
- Average wave energy density of 1,609 J/m^2 of surface waves.
- Spectral width of 0.172.
- Directionality coefficient of 0.74.
- Main direction of incident wave power (with respect to North) is 42° in a clockwise direction
- Withstand the force of associated with a wave of height 21.8 m.

Design life of 30 years with expected probability of a 1 in 100 year return wave at 26%.

AVAILABILITY OF DATA

All data sets used for supporting the conclusions of this article are available on the National Oceanic and Atmospheric Administration (NOAA) National Data Buoy Centre (NDBC) website.

ACKNOWLEDGEMENTS

The authors wish to thank NOAA for the data provided by their buoys located across the Caribbean region on their website. These buoys were instrumental for the calculations performed and results determined. This research did not receive any specific grant from funding agencies in the public, commercial or not-for-profit sectors.

DATA SOURCE

The data gathered and analysed using long-term wave statistic calculations covered the years 2009, 2010, 2011, 2012, 2013, 2014, 2015, 2016, 2017 and 2018. For reference purposes, the buoy data for 41040, 41041, 41043, 41044, 41046, 41052, 41053, 41060 and 41085 can be found at the following link: https://www.ndbc.noaa.gov.

ORCID

Krishpersad Manohar https://orcid.org/0000-0003-2452-2025
Anthony Adeyanju https://orcid.org/0000-0001-5787-0793

REFERENCES

1. United Nations: Transforming Our World: The 2030Agenda for Sustainable Development. The United Nations, New York (2016)
2. Lemessy, K.G., Manohar, K., Adeyanju, A.: A review of wave energy conversion and its place in the Caribbean region. Paper presented at the 13th European wave and tidal energy conference (EWTEC 2019), Napoli, Italy, 1–6 September 2019
3. Lemessy, K.G., Manohar, K., Adeyanju, A.: Reducing the barriers to wave energy harvesting: Review. J. Sci. Res. Rep. 26(2), 107–115 (2020). https://doi.org/10.9734/JSRR/2020/v26i230230
4. Göteman, M., Giassi, M., Engström, J., Isberg, J.: Advances and challenges in wave energy park optimization—A review. Front. Energy Res. 8(8), 26 (2020). https://doi.org/10.3389/fenrg.2020.00026
5. Muzathik, A.M., Wan Nik, W.B., Samo, K.B., Ibrahim, M.Z.: Ocean wave measurement and wave climate prediction of peninsular Malaysian. J. Phys. Sci. 22(1), 77–92 (2011)

6. Mathiesen, M., Goda, Y., Hawkes, P.J., Mansard, E., Martin, M.J., Peltier, E., Thompson, E.F., Van Vledder, G.: Recommended practise for extreme wave analysis. J. Hydraulic Res. 32(6), 803–814 (1994). https://doi.org/10.1080/00221689409498691
7. Reeve, D., Chadwick, A., Fleming, C.: Coastal Engineering: Processes, Theory and Design Practice. Spon Press, New York (2004)
8. Ahn, S., Haas, K.A., Neary, V.S.: Dominant wave energy systems and conditional wave resource chracterisation for coastal waters of the United States. Energies 13(3041), 3041 (2020). https://doi.org/10.3390/en13123041
9. Ahn, S., Neary, V.S.: Non-stationary historical trends in wave energy climate for coastal waters of the United States. Ocean Eng. 216(2020), 108044 (2020) https://doi.org/10.1016/j.oceaneng.2020.108044
10. Henry, L., Bridge, J., Satahoo, K., Miller, H., Lougheide, B., Garbutt, D.: Equator-friendly ocean wave energy conversion. In: World Congress on Engineering. IEEE, Piscataway (2016)
11. Appendini, C.M., Torres-Freyermuth, A., Salles, P., López-González, J., Mendoza, E.T.: Wave climate and trends for the Gulf of Mexico: A 30-yr wave hindcast. J. Clim. 27, 1619–1632 (2014). https://doi.org/10.1175/JCLI-D-13-00206.1
12. IEC: IEC TS 62600-101 Marine Energy - Wave, tidal and other water current converters - Part 101: Wave energy resource assessment and characterization. International Electrotechnical Commission (IEC), Geneva (2015)
13. IEC: IEC TS 62600-2 Marine Energy - Wave, tidal and other water current converters - Part 2: Design requirements for marine energy systems. International Electrotechnical Commission (IEC), Geneva (2016)
14. NOAA National Data Buoy Center: Handbook of Automated Data Quality Control Checks and Proceedures. Stennis Space Center, Hancock CountyC (2009)
15. NOAA National Data Buoy Center: Historical NDBC data. https://www.ndbc.noaa.gov/historical_data.shtml. Accessed 4 June 2019
16. NOAA National Data Buoy Center: Measurements and Descriptions of Units. 05 08. https://www.ndbc.noaa.gov/measdes.shtml. Accessed 1 Oct 2020
17. World Meteorological Organisation Secretariat: Guide to Wave Analysis and Forecasting. World Meteorological Organisation, Geneva (1998)
18. BSI: BS 6349-1:2000 Maritime structures - Part 1: Code of practice for general criteria. British Standards Institute (BSI), London (2000)
19. Penalba, M., Ulazia, A., Saenz, J., Ringwood, J.V.: Impact of long-term resource variations on wave energy farms: The Icelandic case. Energy 192(116609), 116609 (2020). https://doi.org/10.1016/j.energy.2019.116609
20. NOAA Atlantic Oceanographic and Meterological Laboratory: Frequently asked questions about hurricanes. https://www.aoml.noaa.gov/hrd-faq/#1569507388495-a5aa91bb-254c. Accessed 19 Oct 2020
21. Herbich, J.B.: Handbook of coastal engineering. McGraw-Hill, New York (2000)
22. Krogstad, H.E., Arntsen, O.A.: Linear Wave Theory Part B: Random Waves and Wave Statistics. University Study. Norwegian University of Science and Technology, Trondehim (2000)
23. Silvestrini, R.T., Burke, S.E.: The Certified Quality Engineer Handbook, 4th ed. ASQ/Infotech, Milwaukee (2017)
24. Gocic, M., Trajkovic, S.: Analysis of changes in meteorological variables using Mann-Kendall and Sen's slope estimator statistical tests in Serbia. Global Planet. Change 100(2013), (2013). https://doi.org/10.1016/j.gloplacha.2012.10.014
25. Ahn, S., Neary, V.S.: Wave energy resources characterization employing joint distributions in fequency-direction-time domain. Appl. Energy 285(2021), 116407 (2021). https://doi.org/10.1016/j.apenergy.2020.116407
26. Maisondieu, C., Boulluec, M.L.: Benefits of using a spectral hindcast database for wave power extraction assessment. Int. J. Ocean Climate Syst. 7(3), 83–87 (2016). https://doi.org/10.1177/1759313116649967
27. Campos, R.M., Soares, G.: Comparison and assessment of three wave hindcasts in the North Atlantic Ocean. J. Operational Oceanogr. 9(1), 26–44 (2016). https://doi.org/10.1080/1755876X.2016.1200249
28. Munk, W.H., Miller, G.R., Snodgrass, F.E., Barber, N.F.: Directional recording of swell from distant storms. Philos. Trans. Royal Soc. London Series A, Math. Phys. Sci. 255, 505–584 (1963)
29. Zheng, C.-W., Chen, Y.-G., Zhan, C., Wang, Q.: Source tracing of the swell energy: A case study of the Pacific Ocean. IEEE Access 7(2019), 139264–139275 (2019). https://doi.org/10.1109/ACCESS.2019.2943903
30. Mofor, L., Goldsmith, J., Jones, F.: Ocean Energy: Technology Readiness, Patents, Deployment Status and Outlook. Industry Report. IRENA, Masdar City (2014)
31. Guanche, R., de Andrés, A., Losada, I.J., Vidal, C.: A global analysis of the operation and maintenance role on the placing of wave energy farms. Energy Convers. Manage. 106, 440–456 (2015)
32. Waters, R.: Energy from Ocean Waves: Full Scale Experimental Verification of a Wave Energy Converter. PhD Dissertation. Uppsala University, Sweden (2008)
33. Arinaga, R.A., Cheung, K.F.: Atlas of global wave energy from 10 years of reanalysis and hindcast data. Renew. Ener. 39, 49–64 (2012)
34. Coe, R.G., Yu, Y.-H., van Rij, J.: A survey of WEC reliability, survival and design practices. Energies 11(4), 4 (2018). https://doi.org/10.3390/en11010004
35. Caires, S., Sterl, A.: 100-year return value estimates for ocean wind speed and significant wave height from the ERA-40 data. J. Clim. 18, 1032–1048 (2005)
36. Alves, J., Henrique, G.M., Young, I.R.: On estimating extreme wave heights using combined Geosat, Topex/Poseidon and ERS-1 altimeter data. Appl. Ocean Res. 25(2003), 167–186 (2004)
37. European Marine Energy Centre: Guidelines for Design Basis of Marine Energy Conversion Systems. British Standards Institute (BSI), London (2009)

How to cite this article: Lemessy, K.G., Manohar, K., Adeyanju, A.: Analysis of the Caribbean wave climate for wave energy harvesting. IET Renew. Power Gener. 15, 3409–3423 (2021). https://doi.org/10.1049/rpg2.12285